Abdou *et al.*
Egyptian Journal of Medical Human Genetics (2022) 23:150
https://doi.org/10.1186/s43042-022-00353-2

Egyptian Journal of Medical Human Genetics

RESEARCH Open Access

Mutational analysis of phospholipase C epsilon 1 gene in Egyptian children with steroid-resistant nephrotic syndrome

Mohammed Abdou[1*], Abeer Ramadan[2], Basma E. El-Agamy[1], Mohamed S. EL-Farsy[3] and Eman M. Saleh[1]

Abstract

Background: Steroid-resistant nephrotic syndrome (SRNS) is characterized by unresponsiveness of nephrotic range proteinuria to standard steroid therapy, and is the main cause of childhood renal failure. The identification of more than 53 monogenic causes of SRNS has led researchers to focus on the genetic mutations related to the molecular mechanisms of the disease. Mutations in the *PLCE1* gene, which encodes phospholipase C epsilon 1 (PLCε1), have been described in patients with early-onset SRNS characterized by progressive renal failure. In this study we screened for *PLCE1* mutations in Egyptian children with SRNS. This is a descriptive case series study aiming to screen for *PLCE1* gene mutations by direct sequencing of five exons—9, 12, 15, 19, 27—in 20 Egyptian children with SRNS who entered the Nephrology Unit, Faculty of Medicine, Ain-Shams University from November 2015 to December 2017. The variants detected were submitted to in silico analysis.

Results: We screened for mutations in five selected exons of *PLCE1* gene. We identified seven variants in the five selected exons with homozygous and heterozygous inheritance pattern, two are intronic variants, two are silent variants, and three are missense variants. We identified four novel variants two are silent with no clinical significance and two are missense with uncertain clinical significance and pathogenic in-silico predictions; one p.Arg1230His in exon 12, the other is p.Glu1393Lys in exon 15.

Conclusions: We identified four novel mutations, findings which added to the registered SNP spectrum of the *PLCE1* gene. These results widen the spectrum of *PLCE1* gene mutations and support the importance of genetic testing in different populations of SRNS patients, therefore, to assess the vulnerability of Egyptian children to SRNS candidate genes, further studies needed on a larger number of cases which undoubtedly provide new insights into the pathogenic mechanisms of SRNS and might help in control of the patient. Additionally, the use of computational scoring and modeling tools may assist in the evaluation of the way in which the SNPs affect protein functionality.

Keywords: Nephrotic syndrome (NS), Phospholipase C epsilon 1 (PLCE1), Steroid-resistant nephrotic syndrome (SRNS), Nonsynonymous single nucleotide polymorphism (nsSNP), Synonymous single nucleotide polymorphism (sSNP)

Background

Nephrotic syndrome (NS) is the main feature of childhood glomerular disease, and is characterized by heavy proteinuria, hypoalbuminemia, and edema [1]. Most children with NS respond well to standard steroid therapy, and are clinically controlled. However, approximately 10%–20% of children are classified as having steroid-resistant NS (SRNS) and progress rapidly to end-stage

*Correspondence: Mohamedabdo_p@sci.asu.edu.eg

[1] Biochemistry Department, Faculty of Science, Ain Shams University, Cairo 11566, Egypt
Full list of author information is available at the end of the article

renal disease (ESRD) [2, 3]. The predominant histopathological pattern of SRNS patients is focal segmental glomerulosclerosis (FSGS) which leads to ESRD in children [4]. In an Egyptian single-center study of 741 Egyptian children, SRNS was found in 43% ($n=354$) of patients, and FSGS histology appeared in 19.2% of SRNS patients [5]. Inherited structural defects of the glomerular filtration barrier were detected in isolated, as well as familial, cases of SRNS [6]. The majority of genes known to cause SRNS are recessive, and SRNS resulting from recessive genes in early childhood involves the genes *NPHS1, LAMB2,* and *PLCE1* [3].

Phospholipase C epsilon 1(PLCε1) (EC.14.3.3) is a member of the PLC enzyme family, and is involved in the hydrolysis of phosphoinositide molecules (phosphatidylinositol 4,5 -bisphosphate (PIP2) into two secondary messengers, inositol 1,4,5 -triphosphate (IP3) and diacylglycerol (DAG), thereby contributing to intracellular signaling. PLCε1, which interacts with several partners, is involved in multiple signaling pathways that can affect gene expression and therefore cell growth and differentiation [7]. Previous studies into *PLCE1* mutations in populations with SRNS showed that *PLCE1* mutations present as an early-onset nephrotic syndrome (NPHS3; 610725) which progresses rapidly to ESRD with diffuse mesangial sclerosis (DMS) histology (truncating or with splice site mutations) or presents in adulthood with FSGS histology with C-terminal truncating or missense mutations. The defect due to the truncation of *PLCE1* leads to a defect in the phosphoinositide metabolic pathway. This defect is a causative agent for kidney disease [8, 9], and is the major cause of isolated DMS [10]. Till now, there is no *PLCE1* screening mutations have been identified in the Egyptian children. In this study we aimed to identify causative mutations of the *PLCE1* gene in exons 9, 12, 15, 19, and 27 in twenty Egyptian children with SRNS and analyze the pathogenicity of these mutations. This study paves the way to further studies to assess the *PLCE1* gene mutational spectrum in large scale within Egyptian population.

Methods

Study subjects

This was a descriptive case series study conducted on 20 patients who entered the Nephrology Unit, Faculty of Medicine, Ain-Shams University from November 2015 to December 2017. NS is diagnosed when there is a urinary protein excretion > 40 mg/m^2 of surface area/hour with urine protein: creatinine ratio (uPCR) > 200 mg/mmol with hypo-albuminemia and edema [11]. The patients were aged between 1 and 16 years old at the onset of the disease, and did not respond to eight weeks of oral treatment with Prednisolone (Predsol Forte® or Solupred®) at a dosage of 2 mg/kg/day [11]. Congenital and familial NS patients with pedigree data were included within the criteria of the study. The criteria for exclusion were steroid-responsive NS or steroid-dependent NS, patients with congenital renal anomalies, and patients with NS secondary to a condition such as infection or lupus. Each participant was informed about the study purpose, and either verbal or some written consent was obtained and signed by family members.

Clinical data and biochemical measurements

Venous blood samples (5 ml) were collected into ethylenediaminetetraacetic acid (EDTA) tubes as part of routine medical procedures involving hospitalization. Some of the blood was subjected to a complete blood count, ESR, liver and renal function tests, urine analysis, and albumin/creatinine ratio. Some renal biopsies were performed by hospital pathology department. The rest of the blood was used for molecular analysis. The molecular analysis was performed at Molecular Genetic and Enzymology department, Human Genetic and Genome Research Institute, National Research Centre, Giza, Egypt.

Genomic DNA extraction, PCR amplification, and DNA sequencing

Genomic DNA was extracted using DNA extraction and purification kits (Qiagen, Hilden, Germany; Cat. No.51304) according to the manufacturer's protocol. Genomic DNA was amplified using Taq PCR master mix (Qiagen; Cat. No. 201443) using intronic primers flanking each of the coding exons of *PLCE1* [9, 12, 15, 19, and 27], with a total volume of 100 µl. Primer sequences and PCR conditions are available on request, and primer sequences as specified in [8] are shown in Table 1. The purified PCR products sequenced using the chain termination method [12], in both directions, using the same primers as used in the PCR amplification process, using Big Dye Termination kits (Applied Biosystems, Foster City, CA, USA). The data were analyzed on an ABI Prism 3500 Genetic Analyzer (Applied Biosystems,) according to the manufacturer's instructions. The DNA sequences were analyzed by visual inspection, using Finch Tv (Geospiza, Denver, CO, USA) to detect heterozygotic positions and exclude the background noise. The sequences were subjected to in silico analysis for SNP annotation.

Statistical analysis

Statistical analysis was done using the statistical package for the social science (SPSS version 22.0) (IBM Corp, NY, USA). Data were expressed as (mean ± SD) for quantitative data. Data were analyzed using

Table 1 The Sequence of PCR primers

Fragment	Sequence (5′-3′)		Annealing TM	Fragment (bp)
PLCE1_Ex9	F	CGGTCAGCCTTAATGTAGGTC	47C°	392
	R	GCTTGCAGAAGTACCTTTAG		
PLCE1_Ex-12–13	F	AATTGGAGCAAGTCTGGTGG	59 C°	502
	R	GTGTGACTGGACCTCTGACC		
PLCE1_Ex-15–16	F	GATGTGGTGGTTTCTTTCCC	58 C°	477
	R	TCAAAGGAGTCTGGGGTCAG		
PLCE1_Ex-19	F	GCTAACGTTCACCCAAGTGT	46C°	465
	R	GCTAAGTGACTGAATTCAGA		
PLCE1_Ex27	F	GCTTATGAAATACCCTCACT	41C°	319
	R	GGCAACTGCTTCTGCTACGG		

Student's t-test as regards normally distributed data. *P* value ≤ 0.05 was considered statistically significant.

Data set

We used BLAST [13] to align our query sequences obtained by Sanger sequencing in abi format aligned against the human reference genome version GRCh38/hg38 from GenBank [14], and identified the differences between the nucleotide sequences of our queries and the reference *PLCE1* gene sequence (GenBank; NG_015799.1). The protein sequence of PLCε1 protein was retrieved in FASTA format from NCBI [15] by protein ID (NP_057425.3) or from Uniprot [16] by Uniprot ID (Q9P212). The human gene nomenclature used follows the standards of the HUGO Gene Nomenclature Committee (HGNC) [17]. Protein structures were downloaded from the PDB database [18]. The variants were named according to #HGVS version 4.1 [19] and using the canonical transcript which consist of 2302 amino acids and designated by ENSMBLE ID ENST00000371380 or the GenBank transcript ID NM_016341.4**.**

Computational analyses

To evaluate the effects of the SNPs, we used a range of computational tools. We predicted the effect of SNPs at the genetic level on gene expression or gene chromatin binding, and at the protein level, where residue substitution may affect protein stability, intra- and inter-molecular interaction patterns, and evaluated the evolutionary conservation of residues. Table 2 shows the tools and their methodologies used to predict the pathogenicity of the obtained SNPs, as well as their effects on protein structure and function.

Homology modeling

We evaluated the effects of amino acid substitutions on the 3D structure of the proteins, which in turn affects the function of the protein. Since a PDB structure for whole sequence of the PLCε1 protein product is not available, we used Modeller 9.23 software, which relies on the satisfaction of spatial restraints obtained from the 3D structures of proteins homologous to the query protein [37]. We selected a specific amino acid sequence of the PLCε1 protein, from positions 1198 to 2117, encompassing the two novel nSNPs identified in this study. Using the PSI-BLASTp database search tool, we searched each domain sequence against the PDB database to obtain well-matched PDB structures [43]. PDB files of highly matched protein domains were used as templates in a Multi template building model to predict the PDB structure of the PLCε1 protein domains that encompass the two novel variants, and to determine the effect of amino acid substitution on the 3D structure. The Modeller program uses Python. The missing loops of the structure obtained were refined using ModLoop [44]. Clashing residues and bad rotamers were fixed using the Swiss-PDB viewer [45] and Chimera. The PDB structure thus obtained was submitted to structural and functional analysis by evaluating the effect of the SNPs on its geometry (root mean square deviation (RMSD) variation) and its interaction pattern.

Results

The study was conducted on 20 patients with SRNS; 13 males and 7 females in a ratio of 1.85:1. The mean age at the time of the study was 6 years. Fourteen patients (70%) showed symptom relief with intensive immunosuppressive therapy such as cyclosporine A (CsA) (Sandimmune®) at a dose of 150 mg/m2/day added to oral

Table 2 Different in silico tools used in prediction of missense variants pathogenecity in PCLE1 gene

Purpose	In silico tools	Methodology	Ref
1-Prediction of deleteriousness of SNP upon nucleotide substitution	**FATHMM-MKL:** Predicts noncoding effects by integrating functional annotation information from the ENCODE. Range 0 to 1	Insert chromosome position, genomic position, wild nucleotide, mutated nucleotide, values above 0.5 are predicted to be deleterious	[20]
	Varsome: Depending on pathogenicity score (DANN) conservative score (GERP) and other prediction scores	Submit SNP by its genomic position and its protein position	[21]
	Mutation taster:	Submit nucleotide substituents within few nucleotides around	[22]
	Trapscore: is a prediction score between 0–1 with Regarding the percentile thresholds above the 90th percentile as possibly damaging and above	Submit SNP by its genomic position according to (GRCh37/hg19) version	[23]
2-The effect of SNP on gene regulation and DNA-chromatin binding	**Consite Server**	Analyze single sequence option, insert genomic sequence of whole exon 20 and 27 nucleotide sequence individually containing the intron/exon boundaries, select Homo sapiens, TF score cutoff is 80%	[24]
3- Prediction of nsSNP deleteriousness acc. to ranking scores upon amino acid change	**PredictSNP0.1** is a consensus classifier that enables access to the nine best performing prediction tools: SIFT, PolyPhen-1, PolyPhen-2, MAPP, PhD-SNP, SNAP, PredictSNP, and nsSNPAnalyzer	Submission of potein ID Q9P212 and substituents as R1230H, E1393K	[25]
	SNP&GO: Disease probability (if > 0.5 mutation is predicted Disease)	Submit Protein sequence and amino acid substitutents	[26]
	Suspect	Submit Protein sequence and amino acid substitutents	[27]
	PROVEAN: -2.5 is consider as a default threshold, therefore, variants with a score equal to or below -2.5 are considered deleterious	Protein sequence and amino acid substitutents	[28]
	FATHMM: Depend on algorithm combines sequence conservation with pathogenicity weights	protein identifier(Q9P212) and amino acid substitutents	[29]
	PANTHER	Protein sequence, substitution and single organism(Homo sapiens)	[30]
4-Prediction of Protein stability change upon amino acid substitution	**I-mutant 2.0**	Submit the whole amino acid sequence and substituents as R1230H, E1393K	[31]
	Mupro	Submit the whole amino acid sequence and substituents as R1230H, E1393K	[32]
	PremPS	Submit PDB file and substituents	[33]
	DynaMut: DynaMut have implemented a consensus estimate of effect upon mutation on protein folding free energy, regarding the environment characteristics of the wild-type residue (e.g., relative solvent accessibility, residue depth and secondary structure) and used in the development of mCSM-Stability and consensus DUET predictions	Submit PDB file and substituents	[34]

Table 2 (continued)

Purpose	In silico tools	Methodology	Ref
5-Estimation of amino acid conservation	**Consurf:** predicts the crucial functional regions of a protein by estimating the degree of amino acid conservation. The grade range from 1 to 9 estimates the extent of conservation of the amino acid	Insert protein sequence	[35]
	WebLogo: conservation can be calculated at each amino acid position that ranges from zero to 4.3 bits (highy conserved)	MSA* file of PLCE1 uploaded for many organisms with their correspnding ID	[36]
6-Molecular modeling	**Modeller9.23 software**		[37]
7-Effect of SNP on protein 3D structure: predict the structural changes introduced by an amino acid substitution	**Missense 3D**	Submit PDB file obtained from and hit the variant site as R1230H	[38]
9-Molecular Geometry visualization	**UCSF Chimera**	1-structure analysis of wild type and both mutated structures 2-Estimate the wildtype PLCE1 PDB structure deviation than mutated forms by using RMSD attribute	[39]
8- Estimation of protein- protein interactions	**Cocomaps**	the PDB file of PLCE1 with chain ID B as molecule 1and IQGAP1 with PDB file 3fay by chain A only as molecule 2	[40]
10- Molecular Docking	**Auto Dock vina**	Using predicted PDB file as a receptor and Pospho-inositide 4,5 diphosphate(Conformer3D_CID_125105.sdf) as a ligand. Docking was carried out with the grid size of 60, 60, and 60 along the X-, Y-, and Z-axis with 0.375 Å spacing	[41]
	Patch Dock server This uses molecular docking algorithm based on structure geometry	Using predicted PDB file as a receptor and Pospho-inositide 4,5 diphosphate(Conformer3D_CID_125105.PDB) as a ligand, Complex Type is protein- small ligand and Clustering RMSD is 1.5 Å	[42]

* multiple sequence alignment

methylprednisone in two divided doses (Predsol®)., while 6 children (30%) were on dialysis. There was no consanguinity between the children.

Clinical and biochemical diagnoses were performed on 20 patients with SRNS and the results matched the criteria for the diagnosis of SRNS patients. Table 3 shows some of the clinical and biochemical data of the patients.

BLAST alignment results

Table 4 and Fig. 1 show a summary of results from the mutation analysis of the *PLCE1* gene. Two SNPs were identified in **Exon 27.** One was novel heterozygous non sense g. 94313289 T > A, T2013T in one case (5%) and one was an intronic SNP g.96072977G > A rs759855980 appeared in five cases (25%)**. Exon 9** contained a novel heterozygous non sense variant c. 3595 G > T hetero G1120G in one case(5%). **Exon 12** had a novel heterozygous nSNP (c.3689G > A) with the codon change R1230H appeared in two cases (10%) one of them was subjected to dialysis. **Exon 15** had a novel heterozygous nSNP (c.3253G > A) with the codon change E1393K in one case (5%). In **Exon 19** two previously reported SNPs were detected: one heterozygous intronic SNP c.3871 + 40C > T with dbSNP id (rs2274225) appeared in seven cases (35%) and another nsSNP variant c.4724G > C with dbSNP id (rs2274224) with the codon change R1575P appeared in six cases (30%) in homozygous pattern and eight cases(40%) with heterozygous pattern.Figure 2 (A_1 and B_1) shows the flexibility graphs of both residues, colored according to the vibrational entropy change upon mutation

Protein–protein alignment using **BLASTp** indicated that the variant in exon 12 (R1230) is located in a conserved domain designated as Cdd: cd16203 (EF-hand motif found in phosphoinositide phospholipase superfamily) and the variant in exon 15 (R1393) is located in a conserved domain designated as Cdd: cd08596 (Catalytic domain of phosphoinositide-specific phospholipase C-like phosphodiesterases).

Table 3 Clinical and biochemical data of the SRNS patients with *PLCE1* mutations

Parameters	(n = 20) Mean (± SD)
S. Creatinin mg/dl	.5130 (± .08473)
ESR mm/hr	38.8500 (± 6.99078)
Albumin (mg/L)	4.2850 (± .5678)
uPCR mg/mg	3.9300 (± .52123)
Platelets count/microliter × 103	436.3000 (± 157.83472)
TLC cells/mm3 × 103	8.004 (± 1.905)
Hb% g/dl	10.5250 (± .80843)
Age(years)	6 (± 4.8)
ALT unit/dl	35.2000 (± 13.00040)
AST unit/dl	32.9500 (± 9.03487)

All measurements were calculated with p-value ≤ 0.05

Prediction of deleteriousness of SNPs at the nucleotide level

Table 5 shows the results of the prediction of the deleteriousness of SNPs due to nucleotide substitution: according to Varsome, Trapscore, Mutation Taster and FATHMM- MKL results: nsSNP R1230H; g.270037G > A (exon 12) is regarded as a deleterious SNP and probably damaging to the whole protein due to its conservative score, and can affect the splicing site as well as the nsSNP E1393K; g.276866G > A (Exon 15) is predicted as a mutational hot spot site, located in a functional domain, therefore, may be deleterious can affect splicing of the protein

Table 4 A summary of detected SNPs identified using BLAST alignment, and their nomenclature according to the HGVS criteria

Exon	Polymorphism nomenclature	Genetic position (chromosomal position)	Heterozygous/ Homozygous	Patients (n = 20)	Effect on coding	dbSNP id (publication)
9	NM_016341.4:c.3360 T > G	g.265282 T > G, 10:94,254,270-T/G	Heterozygous	1/20(5%)	Non sense p.G1120G	New
12	NM_016341.4:c.3689G > A	g. g.270037 G > A, 10: 94,259,025-G/A	Heterozygous	2/20(10%)	Missense p.R1230H	New
15	NM_016341.4:c.4177G > A,	g.276866 G > A, 10:94,265,854-G/A	Heterozygous	1/20(5%)	Missense p.E1393K	New
19	NM_016341.4:c.4724 G > C	g.285852 G > C, 10: 94,279,840-G/C	Homozygous Heterozygous	6/20(30%) 8/20(40%)	Missense p.R1575P	rs2274224 [46, 47]
	NM_016341.4:c.4795 + 40 C > T	g.290963 C > T, 10:94,279,951-C/T	Heterozygous	7/20(35%)	Intronic	rs2274225 (unpublished)
27	NM_016341.4:c.6004–36 G > C	g.324232 G > A, 10:94,313,220-G/A	Heterozygous	5/20 (25%)	Intronic	rs759855980 (unpublished)
	NM_016341.4:c.6039 T > A,	g.324301 T > A, 10:94,313,289-T/A	Heterozygous	1/20(5%)	Non sense p.T2013T	New

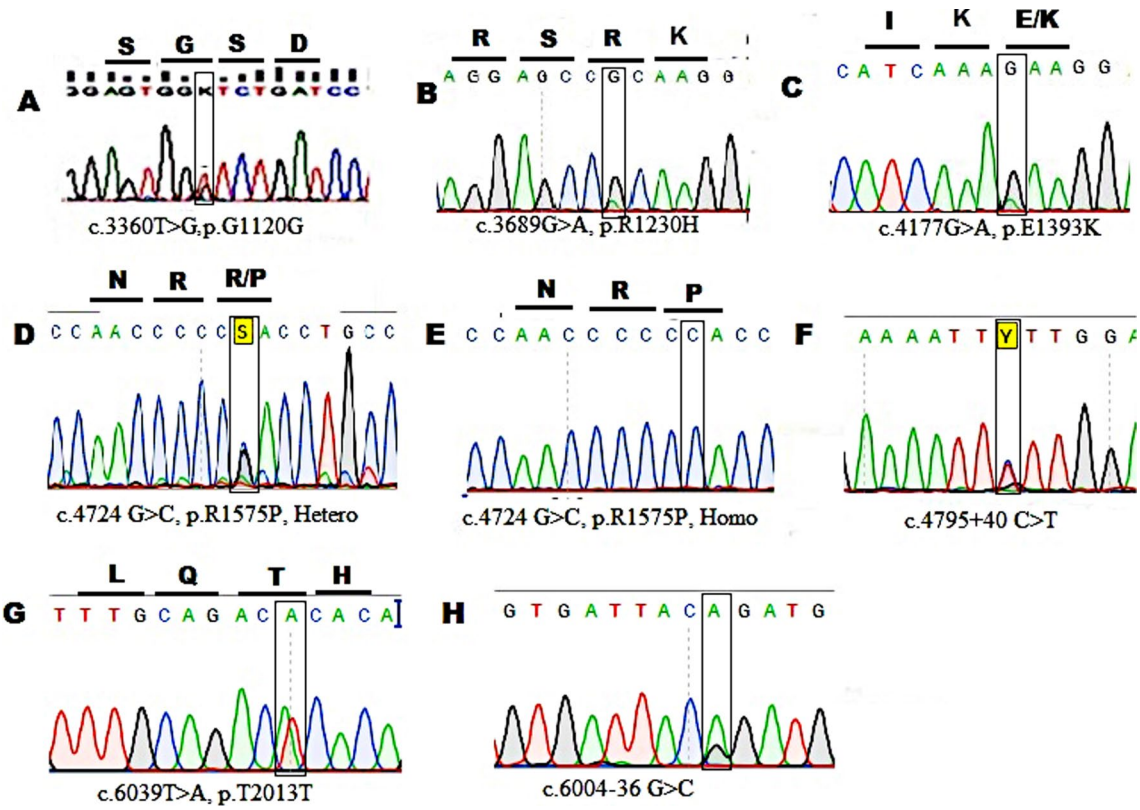

Fig. 1 The chromatograms of obtained variants from direct sequencing and visually inspected by Finch TV. each variant called according to HGVS criteria and ordered in ascending manner from exon 9 to exon 27, where **A** designate the exon 9 non sense SNP **B** designate the exon 12 missense SNP **C** designate the exon 15 missense SNP **D** designate the exon 19 heterozygous missense SNP **E** designate the exon 19 homozygous missense SNP. **F** designate the intronic SNP in exon 19. **G** designate the non sense SNP in exon 27. **H** designate the intronic SNP in exon 27; Each vertical rectangle mark the location of SNP and each codon change leading to amino acid change designated by upper line with the codon and its relative amino acid

accotding to Varsome, Mutation Taster, ans FATHMM-MKL. Additionally, the intronic variant (rs759855980) in (Exon 27) is predicted to damage the final protein transcript according to Trapscore only while other scores predicted it as benign.. On the other hand, the variants: nsSNP R1575P (Exon 19), sSNP g. 94313289 T > A (T2013T), sSNP G1120G: g.265282 T > G (Exon 9) and intronic variant (rs2274225); g.290963C > T(Exon19): predicted to be simple nucleotide substitution without any deleterious effect on transcription or splicing.

Estimation of the effect of intronic SNP on gene regulation and DNA-chromatin binding

DNA genetic regions can be classified into functional and regulator regions. Gene regulation involves the regulation of gene expression and the chromatin binding affinity; genetic variation may alter this regulatory process. We used prediction algorithms to evaluate the effect of intronic SNPs on genetic regulation. The Consite server indicated that intronic SNPs can alter the DNA binding affinity toward different transcriptional factors, and may affect the transcription process, and thus protein expression (Table 6).

Prediction of nsSNP deleteriousness

Tables 7 and 8 show the predictions of the effects of nsSNPs on protein function produced by different scoring tools. Many prediction scores (10/14) evaluated R1230H SNP as a deleterious variant which may be disease causing. While a few prediction scores (6/14) evaluate E1393K SNP as disease causing, the majority of predictions evaluate it as a tolerated variant. The other nsSNP in exon 19 is previously recorded (rs 2,274,224) and predicted as tolerated [46, 47]. This nsSNP has been reported to be related to *PLCE1* mutations implicated in esophageal squamous cell carcinoma in a Chinese population [48].

Evaluation of protein stability

Table 9 shows the prediction of the effects of amino acid substitutions upon protein stability by calculation of

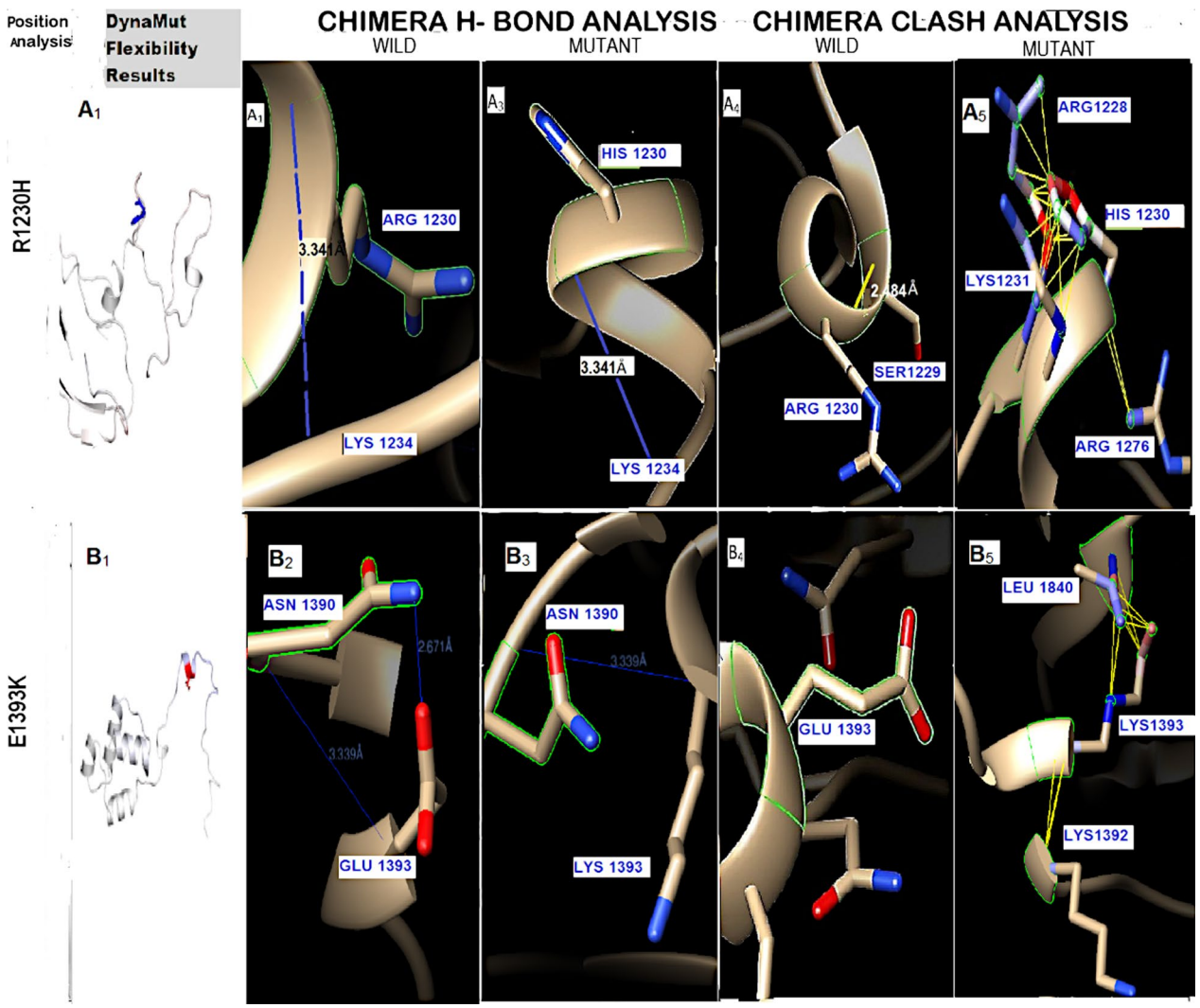

Fig. 2 Molecular Visualization and Analysis of Wild and Mutant positions: (**A**$_1$, **B**$_1$) resemble the DynaMut graphs flexibility results which reveal the SNP positions (**A**$_1$) R1230H (**B**$_1$)E1393K where BLUE increase flexibility and RED decrease flexibility (**A**$_2$(1230), **B**$_2$ (1393))resemble the inter-molecular H- bonding of wild residues (**A**$_3$(1230), **B**$_3$(1393)) resemble the inter-molecular H- bonding of Mutant residues (**A**$_4$(1230), **B**$_4$(1393)) resemble the inter-molecular Clashes of wild residues (**A**$_5$(1230), **B**$_5$(1393)) resemble the inter-molecular Clashes of Mutant residues

Gibbs free energy change according to sequence variation; Table 10 shows the predictions of amino acid substitution upon protein stability by calculation of Gibbs free energy change according to the 3D structure variation. The ΔΔG value is calculated from the difference of unfolding the Gibbs free energy value of the mutated and wild type proteins in Kcal/mol, with an ΔΔG > 0 meaning stabilizing and ΔΔG < 0 meaning destabilizing. The sequence-based predictors, I-Mutant and Mupro, predicted that residue substitution at R1230H and E1393K destabilizes the whole protein. The other structure-based stability predictors differed. DynaMut predicted that R1230H destabilizes and E1393K stabilizes the protein, based on an analysis of deformation energy (a measure of the amount of local flexibility in the protein) and atomic fluctuation (the amplitude of the absolute atomic motion), The ENCOM server estimates the effects of single point mutations on protein dynamics and thermo-stability resulting from vibrational entropy changes. Its analysis of mutant R1230H showed that the Vibrational Entropy Energy ($\Delta\Delta S_{Vib}$) ENCoM was 0.222 kcal mol^{-1} K^{-1}, indicating an increase in molecule flexibility and decrease of protein stability. Mutant E1393K had a ΔΔSVib ENCoM of − 0.043 kcal.mol^{-1}. K^{-1}, indicating a decrease in molecule flexibility and, hence an increase in protein stability. PremPs indicated

Table 5 Prediction of deleteriousness of SNP upon nucleotide substitution

Mutation	Trap Score	Varsome			FATHMML-MKL	Mutation Taster
		GREP	DANN	REVEL		
G1120G (Novel)	0.062 benign	- 1.97	0.7419		Coding score 0.2837	0.999999999997818 disease causing
R1230H (Novel)	0.359 deleterious	5.7699 conseved	0.9994	0.605 pathogenic	Coding score 0.9937	0.99999490647148 disease causing
E1393K (Novel)	0.075 benign	5.9699 conseved	0.9986 pathogenic	0.208 benign	Coding score 0.9837	0.99040168642085 disease causing
R1575P rs2274224	0.045 benign	5.53	0.6793	0.079 benign	Coding score 0.05564	0.999999910833424 simple amino acid change, SNP
rs2274225	0.06 benign	5.53	0.5286 benign		Non-coding score 0.27012	0.999999355568395 without splice site change
rs759855980	0.25 benign	1.97	0.6348		Non-coding score 0.21292	0.99999991390954 With splice site change
T2013T	0.004	0.425				

Non-coding:(positions in intergenic regions, introns or non-coding genes), coding: (positions within coding-sequence exons). GERP:Genomic Evolutionary Rate Profiling (GERP): It ranges from -12.3 to 6.17, with 6.17 being the most conserved. DANN Score is a pathogenicity scoring methodology from 0 to 1 being highly damaging. REVEL is a new ENSEMBLE method for predicting the pathogenicity of missense variants 0 to 1, with higher scores reflecting greater likelihood that the variant is disease-causing

Table 6 Consite server results elucidate the effect of SNP on gene regulation

Mutation	Genomic position	Wild type TF* binding affinity (Species)	Score	Predicted Binding site	TF binding affinity after mutation	Score
rs2274225 (exon 19)	g.290963,c.3871 + 40C > T	PAX6 (H.Sapiens)	9.357	c.3871 + 38 to c.3871 + 51 (TTCTTGGATGATTT)	Athb-1	6.726
rs759855980 (exon 27)	g.324232,c.6004-34G > A	PAX6 (H.Sapiens)	11.332	c.6004–39 to c.6004–26 (ATTACGGATGAATG)	Thing1-E47	7.912

* Transcriptional factor

Table 7 Evaluation of the deleteriousness of nsSNPs by the predictSNP1.0 server based on many prediction tools

Mutation	PredictSNP	MAPP	PhD-SNP	PolyPhen-1	PolyPhen-2	SNAP	SIFT
R1230H	Deleterious (0.606973)	Deleterious (0.409295)	Neutral (0.58231)	Deleterious (0.744912)	Deleterious (0.811429)	Neutral (0.554397)	Deleterious (0.792808)
E1393K	Neutral (0.653073)	Neutral (0.642291)	Deleterious (0.607981)	Neutral (0.668841)	Neutral (0.711712)	Neutral (0.554397)	Deleterious (0.429699)

Table 8 Prediction of nsSNP deleteriousness by another different ranking scores

Mutation	FATHMM	SIFT	PROVEAN	SNPs&GO	PANTHER	Mutpred	Suspect	SNP analyzer
R1230H	0.23 tolerated	0.0 damaging	− 4.128 deleterious	0.683 Disease	0.554 Probably damaging	0.637 Gain of ubquitina-tion	34% benign	Disease
E1393K	0.55 tolerated	0.04 damaging	− 2.662 deleterious	0.194 Neutral	0.220 Probably damaging	0.570 Gain of methylation	23% benign	Disease

Table 9 Sequence-based stability predictions

Mutation	I-mutant2.0	Mupro
R1230H	ddG – 1.3 decrease stability	ddG = -1.412120 Decrease stability
E1393K	ddG – 0.6 decrease stability	ddG = -1.02738 Decease stability

that the stability of the protein increased with both mutations.

Estimation of position conservation

The estimation of the position conservation of specific residues is important when estimating a residue's evolutionary functionality, and can be predicted using WebLogo and Consurf.Figure 3 shows the Consurf results. The conservation score of R1230 was 9 and

Table 10 Structure-Based stability Predictions

Mutation	PremPS (ΔΔG)	DYNAMUT	ΔΔG mCSM	ΔΔG SDM	ΔΔG DUET	$\Delta\Delta S_{Vib}$ ENCoM
R1230H	1.68 kcal/mol (Stabilizing) Core location	− 0.529 kcal/mol (Destabilizing)	− 1.450 kcal/mol (Destabilizing)	0.890 kcal/mol (Stabilizing)	− 1.178 kcal/mol (Destabilizing)	0.222 kcal.mol-1.K-1 (Increase of molecule flexibility)
E1393K	0.4 kcal/mol (Stabilizing) Surface location	0.156 kcal/mol (Stabilizing)	0.171 kcal/mol (Stabilizing)	− 1.000 kcal/mol (Destabilizing)	0.387 kcal/mol (Stabilizing)	− 0.043 kcal.mol-1.K1 (Decrease of molecule flexibility)

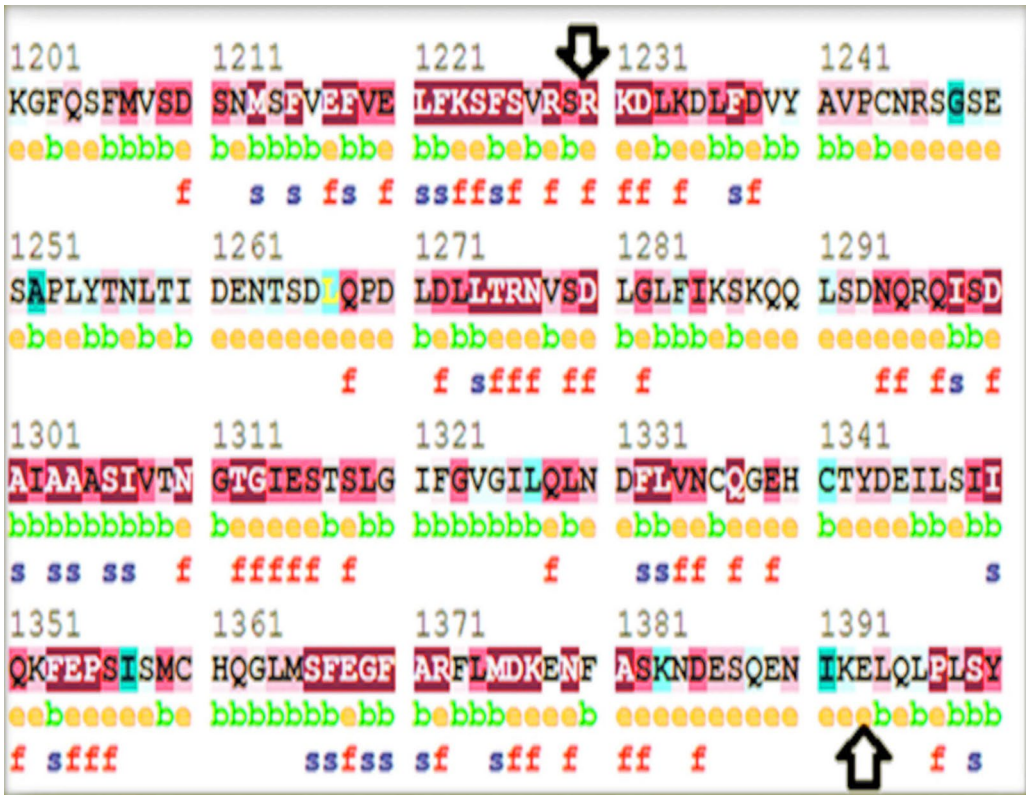

Fig. 3 The conservation score obtained according to Consurf prediction score. The arrows indicating the position of two novel mutations at R1230 and at E1393. Symbol characters (e) indicate the amino acid position is exposed (f) indicate that the amino acid position is predicted functional residue (highly conserved and exposed). b indicate that the amino acid position is a buried residue (s) indicate that the amino acid position is predicted structural residue (highly conserved and buried)

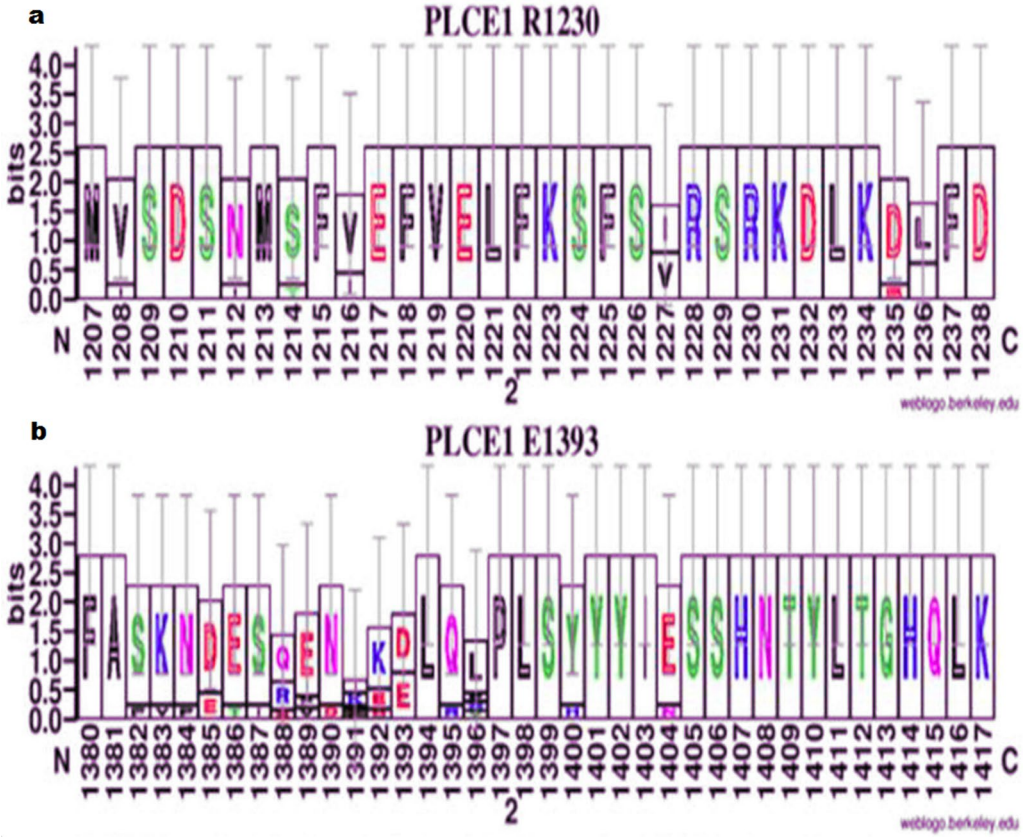

Fig. 4 The WEBLOGO representation of amino acid conservation: input data as Clustal format according to multiple sequence alignment of PLCE1 between human and other organisms. 60 amino acids for PLCE1 protein(Q9P212) Homo sapiens (NP_057425.3), along with seven proteins from Gallus gallus(XP_015144344.2), Canis lupus familiaris (NP_001130037.1), Mus musculus (NP_062534.2), Rattus norvegicus (NP_446210.1), Pan troglodytes (XP_009457233.3) and Danio rerio (NP_001155125.1) and (even in PLC210 the most primitive othologe of PLCE1) Caenorhabditis elegans (AAC38963.1) **a** represent the logo representation of aligned positions containing R1230 (according to human sequence) While **b** represent the logo representation of 60 amino acids of the same organisms but in position containing the other mutant amino acid E 1393 (according to human sequence) show low conservation score than R1230

the symbol was f, meaning it is highly conserved and functional, while E1393 has a score of 5 and symbol e, meaning it is a moderately conserved and exposed residue. Figure 4 also shows the WebLogo results, which indicate that the R1230 position is highly conserved. The overall height of its stack indicates the sequence conservation at this position takes 2.4 bits, and the height of the R symbol within the stacks reflects the relative frequency of the corresponding amino acid at that position between different species. Position E1393 showed a moderate stack height and lower bits.

Homology modeling

Figure 5 shows the PDB structure created, which has three chains that resemble three conserved domains in the PLCε1 protein, as follows: the sequence from 1199 to 1392 resembles the EF-Hand domain, that from 1393 to 2005 resembles the catalytic domain of phosphoinositide-specific phospholipase C-like phosphodiesterases, and that from 2006 to 2117 resembles the RA1 RAS binding domain. The structure was visualized using Chimera. Figure 6 shows the Ramachandran plot of this PDB structure, and its quality and validity was verified using PROCHECK [49].

Effect of SNP on protein 3D structure: prediction of the structural changes introduced by an amino acid substitution

We estimated the effect of the SNPs on the 3D structure of the protein, according to the structure deformation and variation in interaction patterns. Missense3D indicated that substitution R1230H leads to a change from an exposed to a buried state where ARG is exposed

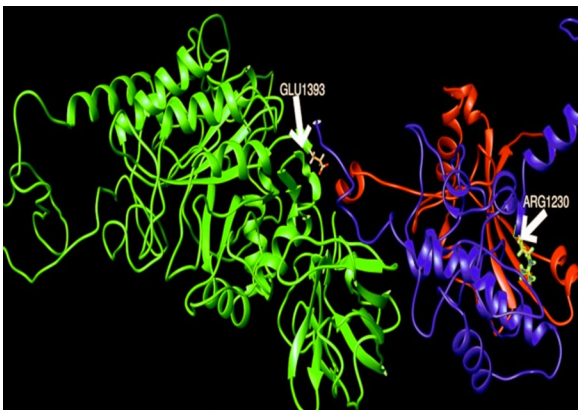

Fig. 5 The modeled 3D structure presicted by modeller 9.23 and viewed by UCSF chimera. The 3D structure appeared as a trimer (3 chains: A,B,C) chain A (Blue colored), Chain B(Green colored) and chain C(Red coolorred) and labelled by the positions of the two amino acids comprising the obtained two novel SNP at R1230 (in Chain A)and E1393(in chain B)

(RSA 36.2%) and HIS is buried (RSA 8.6%). (RSA < 9% for buried and the difference between RSA has to be at least 5%). The Missense3D predictor concluded that the R1230H substitution leads to protein structural damage without altering the secondary structure 'I' (5-turn helix). E1393K was not predicted to lead to any structural damage.

Molecular visualization

Molecular visualization and 3D structure analysis was performed using Chimera software [40]. The superposing feature (structure comparison) between the wild type modeled PLCε1 protein and the modeled mutated forms at positions 1230 and 1393 showed an overall RMSD equal to 0.00, indicating no deviation between the wild and mutated structures. The differences in interaction patterns between the wild type and mutated structures were analyzed using the Rotamer feature of Chimera. Figure 6 and Table 11 show that there was no change in

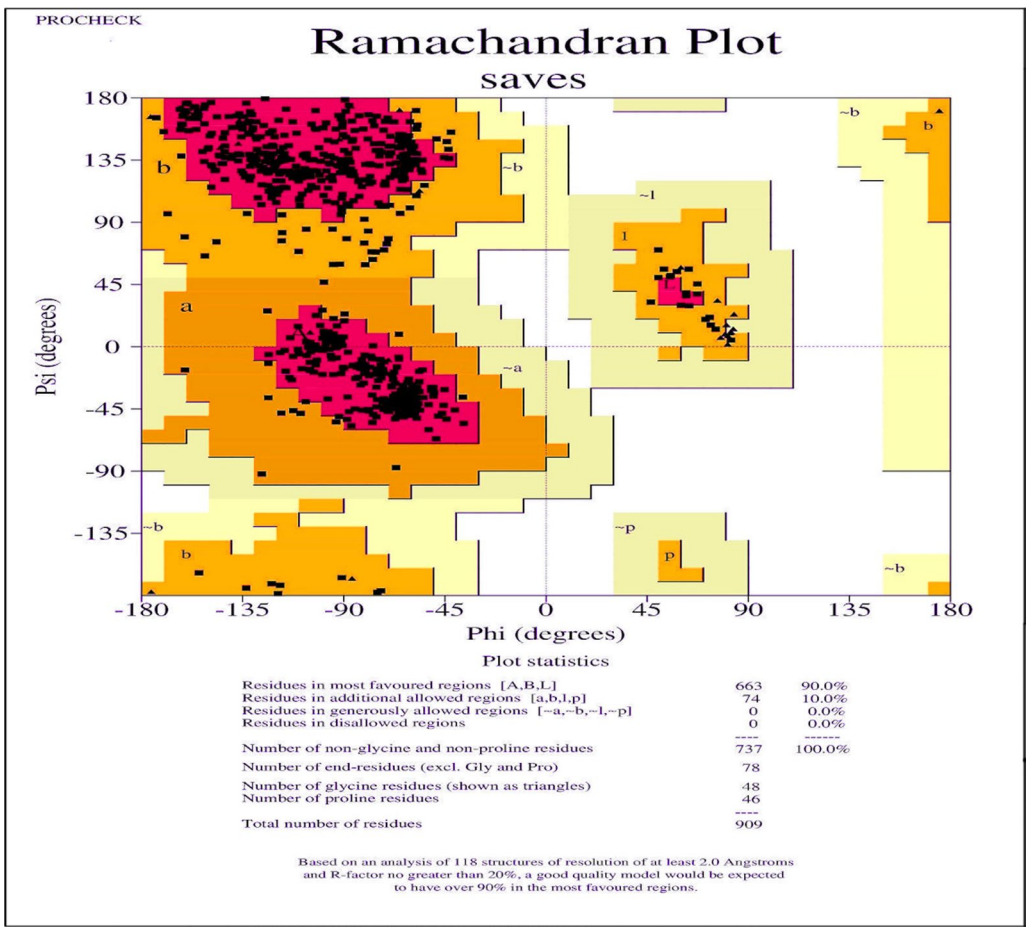

Fig. 6 Evaluation & Validation of predicted PDB model: where the Ramchandran Plot revealed that 90% of all modeled residues lie energetically in the most favored regions. According to PROCHECK server

Table 11 Inter-molecular H- bonding and Clash Analysis of Wild and mutant structure of modeled PLCε1 according to chimera

Position/analysis	1230		1393	
	Wild	Mutant	Wild	Mutant
H-Bonding analysis	1 H-bond with Lys 1234 with distance = 3.241 Å	1 H-bond with Lys 1234 with distance = 3.241 Å	2 H- bonds found with ASN 1390 distance 2.671 and 3.339 Å	1 H-bond found with ASN 1390 3.339 and the another H- bond lost
Inter-molecular Clashes analysis	1 clash found with SER 1229 with distance2.484 Å	20 clashes found with ARG1276, ARG1228, and LYS1231	No clahes found	20 clashes found with LEU 1840 and LYS1392

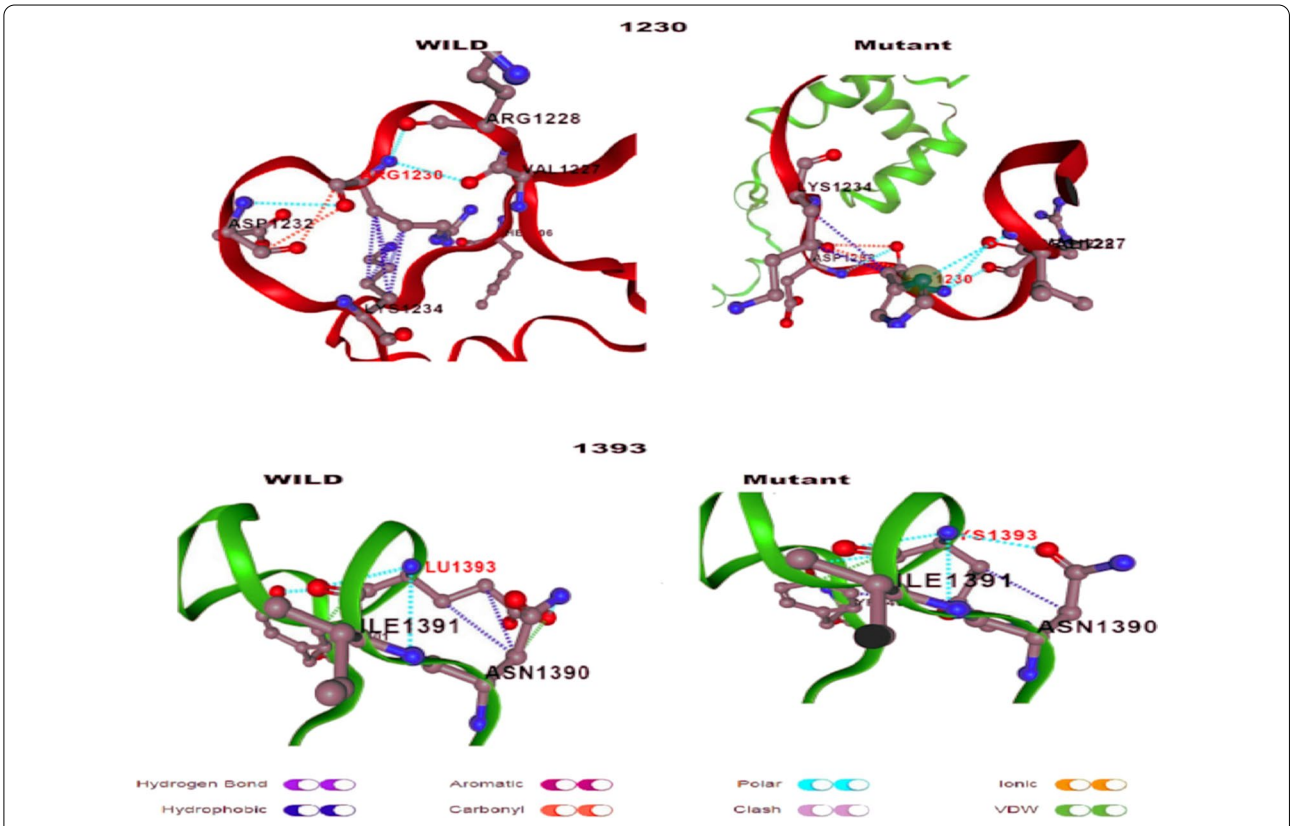

Fig. 7 Intra-molecular Interactions analysis by using PremPs server: The tow interesting sites 1230 with wild (ARG) and mutant (HIS) intearctions with adjacent residues (VAL 1227, ARG 1228, ASP 1232, PHE 2006 and LYS 1234) and 1393 with wild (GLU) and mutant (LYS) interactions with adjacent residues (ASN 1390 and ILE 1391). Each type of interaction have its specific graphical color and appeared as line dots

H-bonding pattern upon R1230H mutation, while the E1393K mutation led to the loss of one H-bond between LYS1393 and ASN1390. Inter-molecular clash analysis showed an increase in clashes of H1230 and K1393 in comparison with the wild type residues R1230 and E1393, respectively. (Note: Chimera analysis criteria: H-bonding analysis, constraints relaxed by 0.4 angstroms and 20 degrees; and Clash analysis, allowed overlap: −0.4, H-bond overlap reduction: 0).

Estimation of protein–protein interactions

DynaMut and PremPs were used to compare non-covalent interactions between wild type and mutant residues, with adjacent residues showing exchange between this. The production of different interactions leads to destabilization of the protein upon R1230H mutation, according to DynaMut, and stabilization of the protein when both mutations occur, according to PremPs. Figure 7 shows the interaction pattern of the PLCε1 PDB

Table 12 The results of interaction prediction of wild type and mutant forms of PLCE1 with IQGAP1

Interacting molecules	Number of interacting residues Molecule1	Number of interacting residues Molecule2	Number of hydrophilic-hydrophobic interaction	Number of hydrophobic-hydrophobic interaction	Number of hydrophilic-hydrophilic interaction
Wild Type PLCE1 and 3fay.pdb	461	318	3521	1529	1973
PLCE1 mutated at R1230H and 3fay.pdb	461	318	3511	1527	1976
PLCE1 mutated at E1393K and 3fay.pdb	461	318	3511	1527	1978

structures, both wild type and mutated at R1230H and E1393K, according to PremPs predictions. Furthermore, interactions between modeled structure of PLCε1 and IQGAP1 PDB structure was computationally evaluated before and after mutations at the two positions. Table 12 shows the CoCoMaps interaction results according to the extent of structure hydrophobicity or hydrophilicity upon mutation. The interaction between PLCε1 and IQGAP1 was predicted to be interrupted by the mutation.

Molecular docking

To further evaluate the changes in interaction pattern induced by mutations, we used molecular docking to estimate the effect of amino acid substitution on the interactions of the protein with small molecules, even when the mutations were not in the active site. We used Auto Dock Vina to estimate the interactions between the modeled structures of the wild type and mutated structures of PLCε1 as an enzyme (receptor) and its substrate, phosphatidylinositol 4,5-diphosphate(PIP_2), and examine

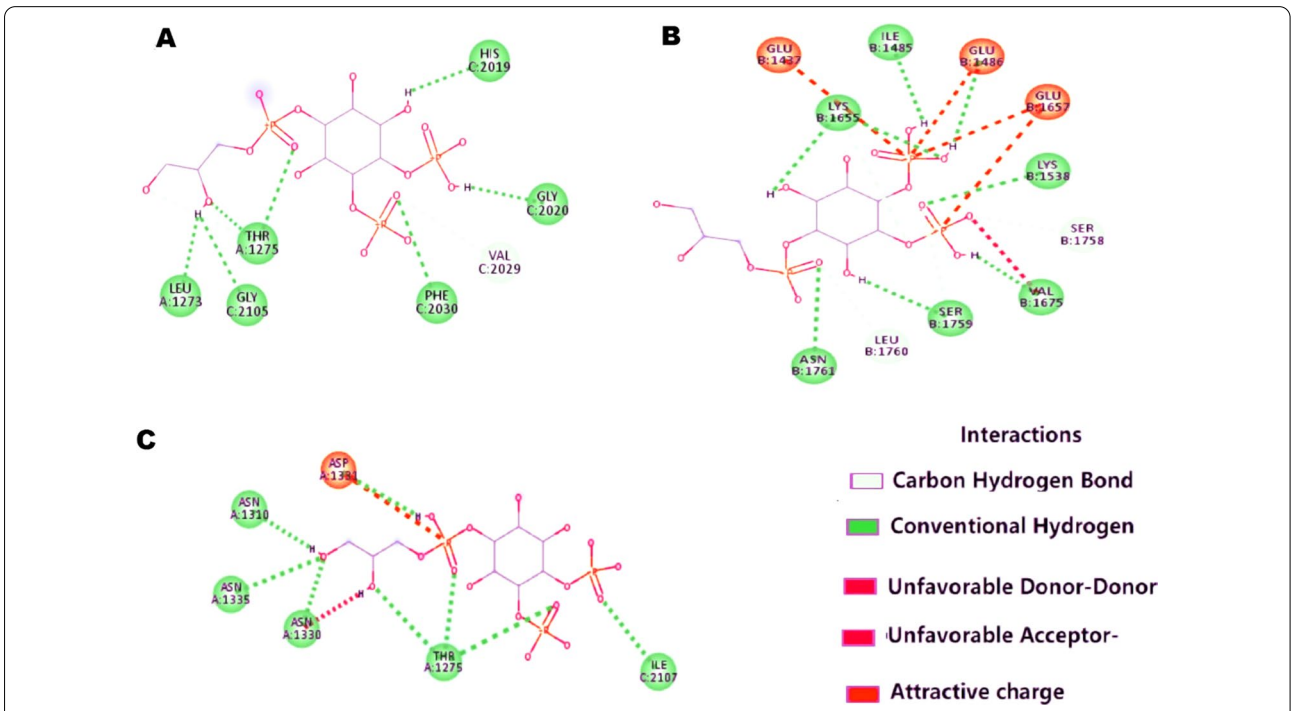

Fig. 8 Auto Dock Vina results analysis of wild and mutated structures: The ligand (PIP_2) appeared in the center of the structure(as sticks) surrounded by the adjacent protein residues in the docking pocket appeared in green circles where **A** wild type docing result **B** mutant R1230H docking results **C** mutant E1393K docking result

Table 13 Summary of AutoDock Vina Results

Receptor	Ligand	Binding energy (Kcal/mol)	Interacting Residues
Wild PLCE1	PIP_2	−7.3	H 2019, T 1275, L 1273, F 2030,G 2020, V 2029, G 2105
R1230H	PIP_2	−7.1	E1437, V1675, I 1485, E1486, K 1538, E1657,S 1759, S 1758, K1655, L 1760, N 1761
E1393K	PIP_2	−7.5	D 1331, T 1275, N 1310, N 1330, N 1335, I 2107

Table 14 Docking results of modeled PDB of PLCε1 with PIP_2 using Patchdock

Receptor	Ligand	Score	ACE
WILD	PIP_2	5058	40.36
R1230H	PIP_2	5292	−7.92
E1393K	PIP_2	5058	40.36

whether the mutation of the residues changed the binding affinity and conformation energy. The results were viewed using Discovery Studio 2.5.5 (Accelrys Pipeline Pilot Co.). Figure 8 and Table 13 show the lowest calculated binding energy value of modeled PLCε1 to PIP_2, where the binding energy of the wild type protein to PIP_2 was −7.5 kcal\mol. This agree with modeled mutant PLCε1 at E1393K which show the same calculated binding energy, that is in contrast to modeled mutant PLCε1 at R1230H which had a larger binding energy, of −7.1 kcal\mol with changed binding residues indicate that affecting the docking pocket, and consequently the patterns of interaction.

The docking results were also evaluated using the Patch Dock server. The docking score and atomic contact energy (ACE) of the native and mutant complexes of the predicted structure of PLCε1 and PIP_2 were calculated. Table 14 shows that the docking score of wild PLCε1 was lower than that of mutant R1230H, and the same as that of mutant E1393K. We confirmed that mutant R1230H may lead to deviations in the interaction affinities of the protein.

Discussion

SRNS is challenging for clinicians, because of the difficulty of its prognosis and management. Thirty to forty percent of patients develop ESRD, requiring dialysis and transplantation [50]. The early identification of disease onset can help in resolving this problem. The screening for mutations in SRNS patients provides a decision about whether to complete or stop steroid therapy, and when to consider transplantation and dialysis. Trials of the screening of genetic mutations in candidate genes implicated in SRNS pathogenesis, like *NPHS1, NPHS2,* and *PLCE1,* is recommended in many populations in which the ethnicity and geographic location are important factors in the variation of the histopathologic lesions. Different genetic mutations in different populations make the need for genetic testing and histological pattern determination of different populations valuable for disease prognosis and management. There have been previous studies screening for *NPHS2* mutations in the Egyptian population that showed novel mutations [51, 52]. Therefore, in this study we looked for new mutations of the *PLCE1* gene in Egyptian SRNS patients.

In comparison with the database, the investigation revealed two novel heterozygous missense mutations in exon12 (R1230H) and exon15 (E1393K). Each is computationally predicted to be pathogenic and has a high conservation score, and the two SNPs are in two conserved domains in the PLC superfamily. The R1230 position is highly conserved even in *Danio rerio*, according to Lovric and colleagues, who assert that "the missense mutation is regarded as a disease causing if a position is continuously conserved at least up to *Danio rerio* (Zebrafish)" [53]. Since the relationship between the SNPs and the disease is obscure, this study was dependent on many prediction tools using different methods to predict the effects of nucleotide variants on structural and functional levels. This analysis was performed step by step, from an estimation of the effect of nucleotide substitution on DNA regulation properties and binding affinity, to residue site conservation and the effect of residue substitution on protein stability, to the interaction and docking properties of the protein with its substrate. The mutant R1230H may lead to destabilization of the whole protein and changes in the affinity of the protein to its ligands. The results were confirmed by the high conservation score of this site. The results are based on many in silico prediction methods, but the results need further clinical and laboratory work for further confirmation.

Missense mutations may affect the function and stability of the PLCε1 protein [8], and lead to glomerular sclerosis [54, 55]. The present study is the first to screen for *PLCE1* genetic mutations in Egyptian children by linking computational, molecular, and clinical results, to widen the spectrum of *PLCE1* mutations related to SRNS. We

demonstrated a novel heterozygous mutation in exon 12, c.3689 G > A (R1230H). This finding may be in accordance with the case of a Caucasian boy from a Romanian family who was diagnosed at six months of age with NS, and failed to respond to steroids. Renal biopsy indicated the presence of DMS, and he reached ESRD at 13 months. He had a *PLCE1* missense mutation due to the nucleotide substitution nt3736C > T in exon 12, with the codon change R1246X [56]. Also, there is a registered SNP with dbSNP ID rs778503393 missense variant A/G K1231R (NC_000010.11:g.94259028A > G) (57) with a prediction of pathogenesis matching our novel SNP R1230H in the same domain, indicating that this domain may not be functional, but may affect the protein stability especially it is belonging to a highly conserved domain. This R1230 position may be a mutational hotspot (disease related position), and further in vitro work is needed for confirmation.

A Chinese study showed that the compound heterozygous nucleotide mutation 577G > A, causing codon change V193I, and 2770G > A, causing codon change G924S, altered the function of PLCε1 in a two-year-old Chinese girl with mild mesangial proliferation, who showed resistance to methylprednisolone therapy. She went into complete remission after two weeks of treatment with CsA, a calcineurin inhibitor [58]. These observations are in accordance with our study, which showed a six-year-old boy with two heterozygous mutations in exon 12 and exon 15 had mild focal mesangial disease with minimal change in another set of glomeruli, showed resistance to prednisolone, and entered remission after treatment with both cyclosporine and prednisolone. In another context, a single copy of the heterozygous mutation does not produce FSGS, if the mutation appeared in both parents recessive heterozygous mutations of *PLCE1* can aggravate FSGS histology in combination with other heterozygous mutations in other podocyte genes, a phenomenon called bigenic heterozygosity [59]. Thus, a further study with gene panel technique is needed to evaluate the mutational analysis of candidate genes in these patients.

The study also demonstrated a nonsynonymous SNP in exon19 showing amino acid change R1575P, matching the results of Machuca et al. in 2010 [46]. This mutation was not identified as playing a role in the pathogenesis of SRNS in those patients, and this nsSNP (R1575P) also appeared in a Vietnamese study which showed seven-day-old boy diagnosed with CNS with heterozygous inheritance [47].

Conclusions

We identified and described mutations in the *PLCE1* gene in Egyptian children. To our knowledge, this is the first study to identify mutations in Egyptian patients with SRNS and widens the spectrum of *PLCE1* mutations in children with SRNS. The computational methods used in this study revealed the importance of using a range of algorithms with different prediction capacities to estimate the effect of variations on protein structure and function. These results will encourage other researchers to conduct more analyses of the relationship between *PLCE1* mutations and SRNS phenotypes in Egyptian children, and their prevalence.

Limitations

The limitations of this research study included the need for large scale mutational screening of the *PLCE1* gene in Egyptian children, with comparisons to healthy controls, to evaluate the prevalence of these mutations in our population, and the lack of in vitro protein analysis. In addition, We screened just part of the gene, only five exons, the need to assess the whole PLCE1 exons for full investigation of mutational screening in those patients.

Abbreviations

ACE: Atomic contact energy; DMS: Diffuse mesangial sclerosis; ESRD: End-stage renal disease; FSGS: Focal segmental glomerulosclerosis; HGNC: HUGO Gene Nomenclature Committee; NCBI: National Center for Biotechnology Information; NS: Nephrotic syndrome; RMSD: Root mean square deviation; SAV: Single amino acid variant; SRNS: Steroid-resistant nephrotic syndrome.

Acknowledgements

We thank the patients and volunteers who participated in this study

Author contributions

MA: have done the wet lab research, in-silico research writing of manuscript. AR:collect samples, design the study, supervision of wet lab research. BE: Done the drafting and revision of the manuscript. MS: Clinician who diagnose and select of all participants in the study, follow up patients and providing the clinical data. EM: Given the final approval of the manuscript to be published. All authors read and approved the final manuscript.

Funding

The work didn`t have any funding or grants.

Availability of data and materials

The datasets supporting the results are included within the article. The data that support the findings of this study are available on request from the corresponding author. The data are not publicly available because of privacy or ethical restrictions.

Declarations

Ethical approval and consent to participate

The article contains no research in which animals were used and conducted on human patients, each participant was informed about the study purpose, some verbal consents and some written consents were obtained and signed by the family members according to the organization's ethical guidelines. The research proposal was revised and approved by the ethical committee of the National Research Centre (NRC), Cairo, Egypt (Ethical Approval Number: 19048) and in adherence with the 1964 Helsinki Declaration.

Consent for publication

Not applicable.

Competing interests

The authors declare that they have no competing interests.

Author details
[1]Biochemistry Department, Faculty of Science, Ain Shams University, Cairo 11566, Egypt. [2]Medical genetics and Enzymology Department, Human Genetic and Genome Research Institute, National Research Center, Giza 12622, Egypt. [3]Pediatrics Department, Faculty of Medicine, Ain Shams University, Cairo 11566, Egypt.

Received: 30 March 2022 Accepted: 24 August 2022
Published online: 08 November 2022

References

1. Noone DG, Iijima K, Parekh R (2018) Seminar idiopathic nephrotic syndrome in children. Lancet 392:61–64
2. Zagury A, De OAL, Araujo JA, Helena R, Novaes L, Pinheiro CA et al (2013) Steroid-resistant idiopathic nephrotic syndrome in children: long-term follow-up and risk factors for end-stage renal disease. J Bras Nefrol 35:191–199
3. Warejko JK, Tan W, Daga A, Schapiro D, Lawson JA, Shril S et al (2018) Article whole exome sequencing of patients with steroid-resistant nephrotic syndrome. Clin J Am Soc Nephrol 13:53–62
4. Trautmann A, Lipska-Zietkiewicz BS, Schaefer F (2018) Exploring the clinical and genetic spectrum of steroid resistant nephrotic syndrome: the PodoNet registry. Front Pediatr 6:200
5. Bakr A, Eid R, Sarhan A, Hammad A, Mahmoud A, El-mougy A et al (2014) Pathological profile of biopsied Egyptian children with primary nephrotic syndrome: 15- year single center experience. J Nephrol 27:419–423
6. Hinkes BG, Mucha B, Vlangos CN, Gbadegesin R, Liu J, Hasselbacher K et al (2007) Nephrotic syndrome in the first year of life: two thirds of cases are caused by mutations in 4 genes. Pediatrics 119:907–919
7. Bunney TD, Katan M (2006) Phospholipase C epsilon: linking second messengers and small GTPases. Trends Cell Biol 16:640–648
8. Hinkes B, Wiggins RC, Hildebrandt F, Gbadegesin RA (2006) Positional cloning uncovers mutations in PLCE1 responsible for a nephrotic syndrome variant that may be reversible. Nat Genet 38:1397–1405
9. Sadowski CE, Lovric S, Ashraf S, Pabst WL, Gee HY, Kohl S et al (2015) A single-gene cause in 29.5% of cases of steroid-resistant nephrotic syndrome. Am Soc Nephrol J 26:1279–89
10. Gbadegesin R, Hinkes BG, Hoskins BE, Vlangos CN, Heeringa SF, Liu J et al (2008) Mutations in PLCE1 are a major cause of isolated diffuse mesangial sclerosis (IDMS). Nephrol Dial Transpl 23:1291–1297
11. Lombel RM, Hodson EM, Gipson DS (2012) Treatment of steroid-resistant nephrotic syndrome in children: new guidelines from KDIGO. Pediatr Nephrol 28:409–414
12. Sanger F, Nicklen S, Coulson AR (1977) DNA sequencing with chain-terminating inhibitors. Proc Natl Acad Sci U.S.A. 74:5463–5467
13. Altschul SF, Gish W, Miller W, Myers EW, Lipman DJ (1990) Basic local alignment search tool. J Mol Biol 215:403–410
14. GenBank ® is the NIH genetic sequence database, an annotated collection of all publicly available DNA sequences. Nucleic Acids Research. 2013. https://www.ncbi.nlm.nih.gov/genbank/. Accessed 6 Oct 2018
15. National Center for Biotechnology Information (NCBI). Bethesda (MD): National Library of Medicine (US), National Center for Biotechnology Information. 1988. https://www.ncbi.nlm.nih.gov/protein. Accessed 6 Oct 2018
16 Pundir S, Martin MJ, O'Donovan C (2017) UniProt protein knowledgebase. In: Wu CH, Arighi CN, Ross KE (eds) Protein bioinformatics. Springer, New York, pp 41–55. https://doi.org/10.1007/978-1-4939-6783-4_2
17 Gray KA, Seal RL, Tweedie S, Wright M, Bruford EA (2016) HUGO gene nomenclature committee (HGNC): a review of the new HGNC gene family resource. Human Genomics. https://doi.org/10.1186/s40246-016-0062-6
18. Berman HM, Henrick K, Nakamura H (2003) Announcing the worldwide protein data bank. Nat Struct Mol Biol 12:980–980
19. Dunnen JD, Kelley GG, Frederik PFM (2016) Human genome variant society (HGVS). Human Mutation. http://varnomen.hgvs.org. Accessed 7 Jul 2018
20. Shihab HA, Rogers MF, Gough J, Mort M, Cooper DN, Day INM et al (2015) An integrative approach to predicting the functional effects of non-coding and coding sequence variation. Bioinformatics 31:1536–1543
21 Kopanos C, Tsiolkas V, Kouris A, Chapple CE, Albarca Aguilera M, Meyer R et al (2019) VarSome: the human genomic variant search engine. Bioinformatics 31:761
22 Schwarz JM, Cooper DN, Schuelke M, Seelow D (2014) Mutationtaster2: mutation prediction for the deep-sequencing age. Nat Method 11:361–362
23 Gelfman S, Wang Q, Mcsweeney KM, Ren Z, La CF, Halvorsen M et al (2017) Annotating pathogenic non-coding variants in genic regions. Nat Commun. https://doi.org/10.1038/s41467-017-00141-2
24 Sandelin A, Wasserman WW, Lenhard B (2004) ConSite: web-based prediction of regulatory elements using cross-species comparison. Nucleic Acids Res 32:W249–W252
25 Bendl J, Stourac J, Salanda O, Pavelka A, Wieben ED, Zendulka J et al (2014) PredictSNP: robust and accurate consensus classifier for prediction of disease-related mutations. PLoS Comput Biol. https://doi.org/10.1371/journal.pcbi.1003440
26 Capriotti E, Calabrese R, Fariselli P, Martelli PL, Altman RB, Casadio R (2013) WS-SNPs&GO: a web server for predicting the deleterious effect of human protein variants using functional annotation. BMC Genomics. https://doi.org/10.1186/1471-2164-14-S3-S6
27 Yates CM, Filippis I, Kelley LA, Sternberg MJE (2014) SuSPect: enhanced prediction of single amino acid variant (SAV) phenotype using network features. J Mol Biol 426:2692–2701
28 Choi Y, Sims GE, Murphy S, Miller JR, Chan AP (2012) Predicting the functional effect of amino acid substitutions and indels. PLoS One. https://doi.org/10.1371/journal.pone.0046688
29. Shihab HA, Gough J, Cooper DN, Stenson PD, Barker GLA, Edwards KJ, Day INM, Gaunt T (2013) Predicting the functional, molecular and phenotypic consequences of amino acid substitutions using hidden Markov models. Human Mutat 34:57–65
30 Tang H, Thomas PD (2016) PANTHER-PSEP: Predicting disease-causing genetic variants using position-specific evolutionary preservation. Bioinformatics. https://doi.org/10.1093/bioinformatics/btw222
31. Capriotti E, Calabrese R, Casadio R (2006) Predicting the insurgence of human genetic diseases associated to single point protein mutations with support vector machines and evolutionary information. Bioinformatics 22:2729–34
32. Cheng J, Randall A, Baldi P (2006) Prediction of protein stability changes for single-site mutations using support vector machines. Proteins Struct Funct Genet 62:1125–1132
33 Chen Y, Lu H, Zhang N, Zhu Z, Wang S, Li M, Prem PS (2020) Predicting the impact of missense mutations on protein stability. PLoS Comput Biol. https://doi.org/10.1371/journal.pcbi.1008543
34 Rodrigues CH, Pires DE, Ascher DB (2018) DynaMut: predicting the impact of mutations on protein conformation, flexibility and stability. Nucleic Acids Res. https://doi.org/10.1093/nar/gky300
35 Ng PC, Henikoff S (2001) Predicting deleterious amino acid substitutions. Genome Res. https://doi.org/10.1101/gr.176601
36 Crooks G, Hon G, Chandonia J, Brenner S (2004) WebLogo: a sequence logo generator. Genome Res 14:1188–1190
37. Sali A, Blundell T (1993) Comparative protein modelling by satisfaction of spatial restraints. Mol Biol 234:779–815
38 Ittisoponpisan S, Islam SA, Khanna T, Alhuzimi E, David A, Sternberg MJE (2019) Can predicted protein 3d structures provide reliable insights into whether missense variants are disease associated? J Mol Biol. https://doi.org/10.1016/j.jmb.2019.04.009
39. Pettersen EF, Goddard TD, Huang CC, Couch GS, Greenblatt DM, Meng EC et al (2004) UCSF Chimera - a visualization system for exploratory research and analysis. J Comput Chem 25:1605–1612
40 Vangone A, Spinelli R, Scarano V, Cavallo L, Oliva R (2011) COCOMAPS: a web application to analyze and visualize contacts at the interface of biomolecular complexes. Bioinformatics. https://doi.org/10.1093/bioinformatics/btr484
41. Trott O, Olson AJ (2010) AutoDock Vina: improving the speed and accuracy of docking with a new scoring function, efficient optimization and multithreading. J Comput Chem 31:455–461

42 Schneidman-duhovny D, Inbar Y, Nussinov R, Wolfson HJ (2005) PatchDock and SymmDock: servers for rigid and symmetric docking. Nucleic Acids Res. https://doi.org/10.1093/nar/gki481
43 Altschul SF, Madden TL, Schäffer AA, Zhang J, Zhang Z, Miller W, Lipman DJ (1997) Gapped BLAST and PSI-BLAST: a new generation of protein database search programs. Nucleic Acids Res 25:3389–3402
44 Fiser A, Sali A (2003) ModLoop: automated modeling of loops in protein structures. Bioinformatics. https://doi.org/10.1093/bioinformatics/btg362
45 Guex N, Peitsch MC (1997) SWISS-MODEL and the Swiss-PdbViewer: an environment for comparative protein modeling. Electrophoresis 18:2714–23
46. Machuca E, Nevo F, Loirat C, Niaudet P, Gubler M, Antignac C (2010) Genotype – phenotype correlations in non-finnish congenital nephrotic syndrome. J Am Soc Nephrol 21:1209–1217
47. Lien NTK, Van Dem P, Huong NT, Dien TM, Thuy TTT, Van Tung N et al (2019) The Role of pSer1105Ser (in NPHS1 Gene) and p Arg548Leu (in PLCE1 Gene) with disease status of Vietnamese patients with congenital nephrotic syndrome: Benign or pathogenic ? Medicina 35:102
48. Duan F, Xie W, Cui L, Wang P, Song C, Qu H (2013) Novel functional variants locus in PLCE1 and susceptibility to esophageal squamous cell carcinoma : based on published genome-wide association studies in a central Chinese population. Cancer Epidemiol 37:647–652
49 Laskowski RA, MacArthur MW, Moss DS, Thornton JM (1993) PROCHECK: a program to check the stereochemical quality of protein structures. J Appl Crystallogr. https://doi.org/10.1107/S0021889892009944
50. Joshi S, Andersen R, Jespersen B, Rittig S (2013) Genetics of steroid-resistant nephrotic syndrome: a review of mutation spectrum and suggested approach for genetic testing. Acta pediatrica 102:844–856
51. Zaki M, El-shaer S, Rady S, El-salam MA, Abd-el-salam R, Abdelfattah I (2019) Analysis of NPHS2 gene Mutations in egyptian children with nephrotic syndrome. Maced J Med Sci 7:3145–3148
52. Thomas MM, Abdel-hamid MS, Nabil NM, Emil EG (2018) Genetic mutation in Egyptian children with steroid-resistant nephrotic syndrome. J Formos Med Assoc 117:48–53
53. Lovric S, Ashraf S, Tan W, Hildebrandt F (2016) Genetic testing in steroid-resistant nephrotic syndrome: When and how? Nephrol Dial Transplant 31:1802–1813
54. Boyer O, Benoit G, Gribouval O, Nevo F, Bilge I, Bircan Z et al (2010) Mutational analysis of the PLCE1 gene in steroid resistant nephrotic syndrome. J Med Genet 47:445–452
55 Al-hamed MH, Al-sabban E, Al-mojalli H, Al-harbi N, Faqeih E, Al Shaya H et al (2013) A molecular genetic analysis of childhood nephrotic syndrome in a cohort of Saudi Arabian families. J Human Genet 58:480–9
56. Ismaili K, Wissing KM, Janssen F, Hall M (2009) Genetic forms of nephrotic syndrome: a single-center experience in Brussels. Pediatr Nephrol 24:287–294
57. National Center for Biotechnology Information (NCBI). Bethesda (MD): National Library of Medicine (US), National Center for Biotechnology Information. 1988:https://www.ncbi.nlm.nih.gov/snp/?term. Accessed 6 Oct 2020
58. Lin T, Li J, Wang F, Cao L, Wu J, Tu J et al (2014) A chinese girl with novel PLCE1 mutations and proliferation of the mesangium respondded to Tacrolimus therapy. Asian Pacific Soc Nephrol 19(3):173. https://doi.org/10.1111/nep.12178
59 Löwik MM, Groenen PJ, Levtchenko EN (2009) Molecular genetic analysis of podocyte genes in focal segmental glomerulosclerosis—a review. Eur J Pediatr 168:1291–304

Publisher's Note